Acta Crystallographica Section F
Structural Biology and Crystallization Communications
ISSN 1744-3091

Recombinant production, crystallization and preliminary X-ray analysis of PCNA from the psychrophilic archaeon *Methanococcoides burtonii* DSM 6242

Miranda L. Byrne-Steele,[a] Ronny C. Hughes[a] and Joseph D. Ng[b]*

[a]Laboratory for Structural Biology, Department of Biological Sciences, University of Alabama in Huntsville, Huntsville, AL 35899, USA, and [b]ExtremoZyme Inc., HudsonAlpha Institute for Biotechnology, 601 Genome Way, Huntsville, AL 35806, USA

Correspondence e-mail: ngj@email.uah.edu

Received 29 June 2009
Accepted 13 September 2009

Proliferating cell nuclear antigen (PCNA) is a DNA-clamping protein that is responsible for increasing the processivity of the replicative polymerases during DNA replication and repair. The PCNA from the eurypsychrophilic archaeon *Methanococcoides burtonii* DSM 6242 (MbPCNA) has been targeted for protein structural studies. A recombinant expression system has been created that overproduces MbPCNA with an N-terminal hexahistidine affinity tag in *Escherichia coli*. As a result, recombinant MbPCNA with a molecular mass of 28.3 kDa has been purified to at least 95% homogeneity and crystallized by vapor-diffusion equilibration. Preliminary X-ray analysis revealed a trigonal hexagonal *R*3 space group, with unit-cell parameters $a = b = 102.5$, $c = 97.5$ Å. A single MbPCNA crystal was subjected to complete diffraction data-set collection using synchrotron radiation and reflections were measured to 2.40 Å resolution. The diffraction data were of suitable quality for indexing and scaling and an unrefined molecular-replacement solution has been obtained.

1. Introduction

DNA-replication and DNA-repair processes are vital for the maintenance and transfer of genomic information and are central to the reproduction of an organism at any given temperature. Proliferating cell nuclear antigen (PCNA) is an integral component of the replication machinery and acts as a processivity factor during DNA synthesis. The protein has been described as a ring-shaped sliding clamp that encircles duplex DNA and tethers the replicative DNA polymerases to the genomic template (Moldovan *et al.*, 2007). In addition, PCNAs have many other interacting molecular partners that are involved in DNA repair, post-replicative processing such as cytosine methylation, and cell-cycle regulation (Maga & Hubscher, 2003; Warbrick, 1998). Many of these interacting proteins associate with PCNA *via* their PIP (PCNA-interacting protein) motif, which makes contact with the interdomain-connecting loop (IDCL) of PCNA. Hence, a secondary function of PCNA can be viewed as a sliding platform which enables the association of several proteins with DNA in a nonsequence-specific manner (Warbrick, 2000).

Depending upon the domain of life from which the sliding clamp is derived, PCNA is either a dimeric or trimeric assembly of monomeric subunits. The bacterial clamp, also known as DNA polymerase III β-subunit, consists of a dimeric assembly in which each subunit contains three topologically similar domains (Argiriadi *et al.*, 2006; Kong *et al.*, 1992). In contrast, archaeal and eukaryotic PCNAs assemble into a trimeric rather than a dimeric ring in which each subunit contains two rather than three similar domains (Krishna *et al.*, 1994; Matsumiya *et al.*, 2001; Williams *et al.*, 2006). While the euryarchaeal DNA sliding clamp is typically a homotrimer (Chapados *et al.*, 2004; Matsumiya *et al.*, 2001), the situation is further complicated in crenarchaeota as the PCNA from *Sulfolobus solfataricus* is a heterotrimer composed of three distinct PCNA homologues (Dionne *et al.*, 2003; Dore *et al.*, 2006; Hlinkova *et al.*, 2008; Williams *et al.*, 2006). When fully assembled, all kingdoms of life maintain a DNA sliding clamp with a pseudo-sixfold symmetry; these share an extraordinarily similar structural topology despite having low or no sequence identity.

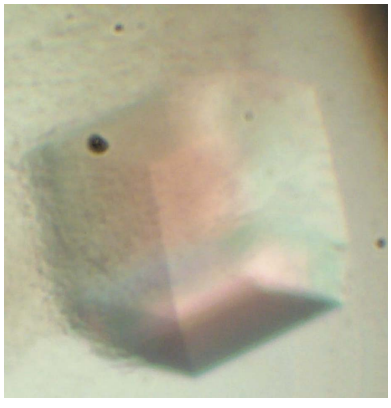

Methanococcoides burtonii DSM 6242 is a eurypsychrophilic euryarchaeota isolated from Ace Lake, Antarctica with a growth range from 271 to 301 K and optimal growth at 296 K (Cavicchioli, 2006; Franzmann *et al.*, 1992). The term eurypsychrophile describes a microorganism that 'likes' permanently cold environments but can tolerate a wide range of temperatures extending into the mesophilic range (Cavicchioli, 2006). Presently, most of Earth's biosphere is perpetually below 278 K and a majority of the ecosystems on Earth (~75%) can be defined as cold, primarily owing to the oceans (Cavicchioli, 2006). Despite the low temperature, these environments are occupied by a myriad of microorganisms including bacteria, archaea, yeast, unicellular algae and fungi (D'Amico *et al.*, 2006; Gerday *et al.*, 2000). Surprisingly, psychrophiles, particularly cold-adapted archaea, have been enormously understudied despite their relevance to fields as disparate as biotechnology and astrobiology (Cavicchioli, 2002; Cavicchioli *et al.*, 2002; Gerday *et al.*, 2000).

The PCNA homolog from *M. burtonii* represents one of the few psychrophilic proteins targeted for structural studies and will be referred to as MbPCNA in the rest of this report. The cloning, heterologous overproduction, purification and initial X-ray analysis of MbPCNA is described here, with the expectation that it will be used for the determination of the first PCNA crystal structure from a cold-adapted archaeon. It is anticipated that the MbPCNA structure will provide insight into both the interactions at domain interfaces and the overall structural stability of one of the central components of the replisome, which supports the process of DNA replication in a cold environment.

2. Materials and methods

2.1. Polymerase chain reaction (PCR) cloning

Genomic DNA for *M. burtonii* DSM 6242 was purchased through the German Resource Center for Biological Material (DSMZ). The MbPCNA open reading frame was amplified by PCR (Mullis & Faloona, 1987) from genomic DNA and cloned into the pET-3a vector to overproduce the protein in fusion with an N-terminal hexahistidine tag. The final amplified MbPCNA product was inserted into the expression plasmid vector by *in vivo* homologous recombination as described by Marsic *et al.* (2008). After transformation using standard molecular-biology protocols (Sambrook *et al.*, 1989), bacterial colonies were randomly selected to inoculate a small-scale liquid culture comprising of 5–10 ml LB containing 100 mg l^{-1} ampicillin at 310 K shaken at 250 rev min^{-1} for 12 h. Plasmids were purified using EZNA plasmid Miniprep Kit II (Omega Bio-Tek, Doraville, Georgia, USA). The sequence of the recombinant MbPCNA-coding region was verified by Functional Biosciences (Madison, Wisconsin, USA).

2.2. Heterologous overproduction

The sequence-verified expression vector containing the properly inserted MbPCNA open reading frame was transformed into competent *Escherichia coli* BL21(DE3)-Rosetta cells (Novagen, Madison, Wisconsin, USA). Transformed cells were mixed with 150 µl LB medium and incubated for 1 h at 310 K. The mixture was then spread on LB–agar plates containing 100 mg l^{-1} ampicillin and 35 mg l^{-1} chloramphenicol. Overnight colonies were then used to inoculate 20 ml LB medium containing 50 mg l^{-1} ampicillin and 35 mg l^{-1} chloramphenicol and grown overnight at 310 K with shaking at 250 rev min^{-1}. The overnight culture was distributed into 2 × 2 l LB medium containing the same antibiotic concentrations and incubation conditions. When the cell density reached an optical density (OD_{600}) of 0.6, the cell cultures were induced with isopropyl β-D-1-thiogalactopyranoside (IPTG) at a final concentration of 1 m*M* and allowed to grow overnight at 291 K. Since the recombinant protein is derived from a cold-adapted archaeon, the temperature was reduced in order to minimize any potential aggregation arising from possible thermal instability of the recombinant protein. The overnight culture was harvested by centrifugation at 3500*g* for 20 min at 277 K.

2.3. Purification

All manipulations were performed at 277 K throughout the purification procedure. Pelleted cells were resuspended in buffer *A* (50 m*M* Tris pH 8.0, 500 m*M* NaCl, 5 m*M* imidazole, 1 m*M* EDTA) and lysed by physical disruption using a Branson Sonifier 250 (VWR Scientific, West Chester, Pennsylvania, USA) for six cycles of 45 pulses. The cell debris was separated by centrifugation at 12 000*g* for 20 min and the remaining supernatant was loaded onto a HiTrap Chelating column (GE Healthcare) charged with Ni^{2+} as per the manufacturer's instructions and pre-equilibrated with buffer *A*. Bound protein was eluted from the column with a 0.05–1 *M* imidazole gradient in buffer *B* (50 m*M* Tris pH 8.0, 500 m*M* NaCl, 1 *M* imidazole, 1 m*M* EDTA) using an ÄKTA Explorer FPLC system (GE Healthcare). Fractions corresponding to the largest peaks were pooled and dialyzed using a 10 000 molecular-weight cutoff Spectrum Spectra/Por dialysis membrane (Spectrum Chemicals, Gardena, California, USA) against ten times the volume of buffer *C* (50 m*M* Tris pH 8.0, 50 m*M* NaCl, 1 m*M* EDTA). The dialyzed solution was concentrated to 2 ml using an Amicon Ultra centrifugal filter device (Millipore, USA), applied onto a Sephacryl S-200 gel-filtration column (Pharmacia, USA) pre-equilibrated with buffer *C* and eluted with the same buffer. Fractions matching the principal peak were pooled and analyzed using SDS–PAGE. The protein was concentrated to 15 mg ml^{-1} as determined by the method of Bradford (1976) for subsequent crystallization trials.

2.4. Crystallization

Sitting-drop vapor-diffusion experiments were performed with the concentrated MbPCNA in order to find initial crystallization conditions. A 96-well format Intelli-Plate (Art Robbins, Sunnyvale, California, USA) was used for the screening process against Crystal Screen I and II (Hampton Research, Aliso Viejo, California, USA) sparse-matrix screens. Each screening sample contained both a 2 µl protein droplet (1:1 volume ratio of protein to reservoir crystallizing solution) and a 3 µl protein droplet (2:1 volume ratio of protein to reservoir crystallizing solution) set to equilibrate against 75 µl of the same reservoir solution. After one month of equilibration at 295 K, crystals were observed in a 3 µl protein droplet with a reservoir solution composed of 0.1 *M* HEPES pH 7.5, 2%(*v*/*v*) PEG 400 and 2.0 *M* ammonium sulfate. The protein crystals obtained were visually observed through a polarized filter under a Nikon visible-light microscope and were photographed with a Kodak Digital Science DC120 camera. Crystals were used directly for X-ray analysis without further optimization.

2.5. X-ray data analysis

X-ray diffraction data were collected from a single crystal using a MAR 300 CCD on the Southeast Regional Collaborative Access Team (SER-CAT) 22-ID beamline at the Advanced Photon Source, Argonne National Laboratory. Crystals were cryoprotected by quick soaking for 10 s in 0.1 *M* HEPES pH 7.5, 2%(*v*/*v*) PEG 400 and 2.0 *M*

ammonium sulfate with the addition of 20% PEG 400 and flash-cooled in liquid nitrogen. Diffraction analysis was performed at 100 K using a crystal-to-detector distance of 200 mm and a 1° oscillation angle. Diffraction data were indexed and reduced with *HKL*-2000 (Otwinowski & Minor, 1997). Data-collection statistics are summarized in Table 1.

3. Results and discussion

The recombinant *E. coli* system used in this investigation produced a yield of approximately 50 mg pure MbPCNA from each litre of growth medium. Purified protein with greater than 95% homogeneity as determined by SDS–PAGE analysis (Fig. 1) was obtained after three chromatography steps. MbPCNA showed an abnormally slow migration on SDS–PAGE corresponding to a molecular mass of 32 kDa, which is slightly larger than the calculated mass of 28.3 kDa based on the amino-acid composition of the recombinant protein with the His tag. Similar irregular electrophoretic behavior has been noted in studies of human PCNA when 11–12% polyacrylamide gels are utilized (Naryzhny *et al.*, 2006; Naryzhny & Lee, 2004). The slower migration of MbPCNA on the gel may be related to anomalous SDS binding or the high acidity of the protein (its calculated pI is 4.5) as reported by others (Garcia-Ortega *et al.*, 2005). However, the principal MbPCNA peak in the elution profile of the size-exclusion purification step corresponded to the expected molecular mass of 28 kDa as measured against standardized molecular-mass markers.

Prismatic MbPCNA crystals with a consistent rhombohedral habit could be obtained within four weeks of vapor-diffusion equilibration. Fig. 2 shows an example of a typical crystal obtained with dimensions of approximately 0.2 × 0.2 × 0.2 mm. The crystals diffracted X-ray synchrotron radiation to 2.40 Å resolution with an $I/\sigma(I)$ of at least 2.8. A representative diffraction image is shown in Fig. 3, revealing a nearly isotropic diffraction pattern with reflection spots having low degrees of mosaicity (∼0.5). Complete data collection was performed using a single crystal belonging to the trigonal hexagonal space group

Table 1
Data-collection statistics.

Values in parentheses are for the highest resolution shell.

Space group	*R*3
Radiation source	SER-CAT 22ID, APS
Unit-cell parameters (hexagonal setting) (Å, °)	$a = b = 102.5$, $c = 97.5$, $\alpha = \beta = 90.0$, $\gamma = 120$
Temperature (K)	100
Wavelength (Å)	1.0
Oscillation range (°)	1.0
Crystal-to-detector distance (mm)	200
No. of frames	180
Resolution range (Å)	25.0–2.40 (2.49–2.40)
Total reflections	53779
Unique reflections	14925
Average redundancy	3.6
$\langle I/\sigma(I)\rangle$	6.2 (2.8)
Overall *B* factor (Å^2)	68.8
Completeness (%)	99.1 (99.8)
$R_{\rm merge}$† (%)	11.7 (45.0)

† $R_{\rm merge} = \sum_{hkl}\sum_i |I_i(hkl) - \langle I(hkl)\rangle| / \sum_{hkl}\sum_i I_i(hkl)$, where $\langle I(hkl)\rangle$ is the mean intensity of reflection *hkl* and $I_i(hkl)$ is the *i*th measurement of the intensity of reflection *hkl*.

*R*3, with unit-cell parameters $a = b = 102.5$, $c = 97.5$ Å. One molecule was assumed to be present in the asymmetric unit, resulting in a Matthews coefficient of 3.52 Å^3 Da^{-1}, corresponding to a solvent content of 64.6% (Matthews, 1968). Data-collection statistics are shown in Table 1 and reveal a notably high *B*-factor value derived from Wilson plot calculations. This may be a consequence of the high thermal motion intrinsic to psychrophilic proteins, as well as the high solvent content as indicated above. Under these circumstances, the relatively high *B* factor may not be entirely unexpected, especially when the maximum resolution is only 2.40 Å. A correct unrefined solution was obtained using *MOLREP* auto molecular replacement from the *CCP*4 program suite (Collaborative Computational Project, Number 4, 1994) and a *CHAINSAW* search model (Schwarzenbacher *et al.*, 2004; Stein, 2008). The search model created by *CHAINSAW* was derived from *Archaeoglobus fulgidus* PCNA (PDB code 1rwz; Chapados *et al.*, 2004) and a *BLAST* sequence alignment (Altschul *et al.*, 1990) of the two PCNAs. The overall correlation coefficient and *R* factor for the correct unrefined solution were 0.60 and 0.48, respectively, using 23.9–2.82 Å data. Examination of the best solution

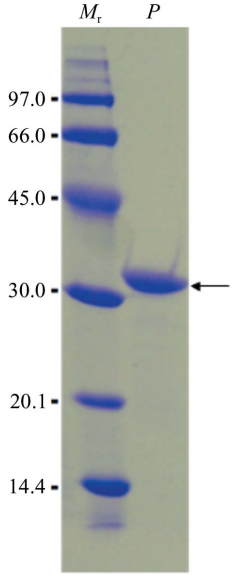

Figure 1
SDS–PAGE analysis of purified recombinant MbPCNA. Approximately 15 µg protein was analyzed on 12% polyacrylamide gel and stained with Coomassie Brilliant Blue. Purified MbPCNA (lane *P*) is indicated by the arrow and compared against molecular-mass standards (lane M_r). The purity of the recombinant protein is observed to be higher than 95%.

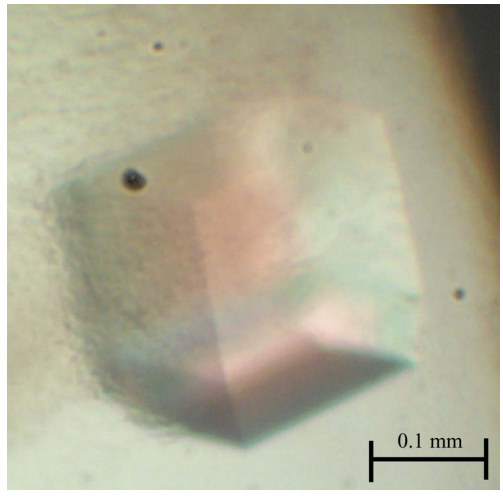

Figure 2
A representative crystal of recombinant MbPCNA protein. A prismatic crystal with rhombohedral habit obtained by vapor-diffusion equilibration against 0.1 *M* HEPES pH 7.5, 4%(*v*/*v*) PEG 400 and 2.0 *M* ammonium sulfate is shown. The dimensions of the crystals were approximately 0.2 × 0.2 × 0.2 mm as measured under a light microscope.

revealed good crystal packing and no clashes between symmetry-related molecules. Despite the high *B* factor, an initial model accounting for over 95% of the backbone of the protein molecule can be clearly traced from a Fourier difference electron-density map (data not shown). Refinement of MbPCNA is in progress and details of the structure will be reported elsewhere.

4. Conclusion

The successful overproduction of recombinant MbPCNA has allowed the crystallization of the first PCNA from a psychrophilic microorganism, specifically a psychrophilic archaeon. The crystals were suitable for X-ray diffraction and a complete X-ray data set was used to produce an initial unrefined model of MbPCNA. To date, only a handful of psychrophilic protein structures have been determined (51 structures deposited in the RCSB PDB as of 30 June 2009) and none of these are of a PCNA homolog. The results reported here will allow comparative structural studies of psychrophilic MbPCNA and its mesophilic and thermophilic homologs. By this, structural information such as the inter/intramolecular hydrogen bonds, secondary-structure content, protein–solvent interactions and solvent accessibility can be compared among PCNAs from representative organisms with different optimal growth temperatures. Ultimately, the important molecular features for thermophilicity and stability may be better understood.

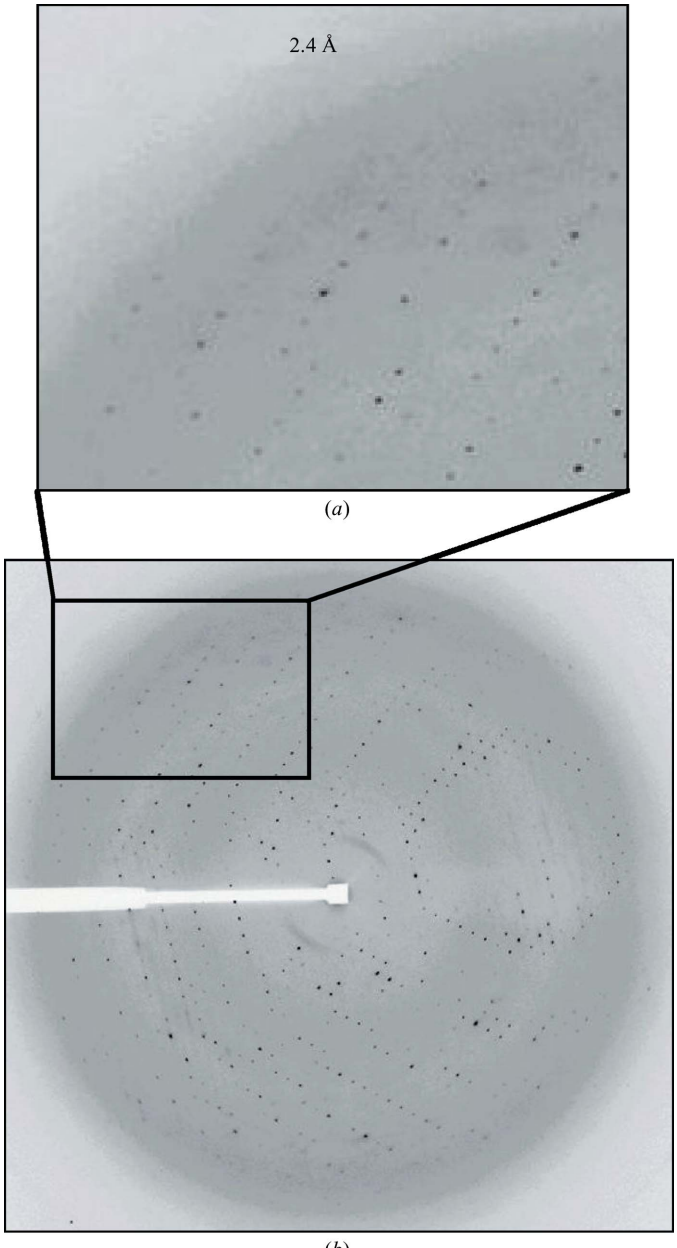

Figure 3
A typical 1° oscillation image obtained during data collection from a single MbPCNA crystal. Reflections were measured to 2.40 Å resolution at the outer edge (*a*) with $I/\sigma(I)$ greater than 2.8. The complete image shows nearly isotropic diffraction (*b*).

MLB-S and RCH were supported by a fellowship from the Alabama EPSCoR Graduate Research Scholars Program (24229), which is funded by the Alabama State Legislature through the Alabama Commission on Higher Education. Additional funding was provided through a National Science Foundation EPSCoR grant (EPS-0447675). We thank Norie Sugitani for her assistance in protein purification and crystallization setups. We also thank Edward Meehan and Damien Marsic for their valuable discussions and input on this project. X-ray data were collected on Southeast Regional Collaborative Access Team (SER-CAT) 22-ID beamline at the Advanced Photon Source, Argonne National Laboratory. Use of the Advanced Photon Source was supported by the US Department of Energy, Office of Science, Office of Basic Energy Sciences under Contract No. W-31-109-Eng-38.

References

Altschul, S. F., Gish, W., Miller, W., Myers, E. W. & Lipman, D. J. (1990). *J. Mol. Biol.* **215**, 403–410.
Argiriadi, M. A., Goedken, E. R., Bruck, I., O'Donnell, M. & Kuriyan, J. (2006). *BMC Struct. Biol.* **6**, 2.
Bradford, M. M. (1976). *Anal. Biochem.* **72**, 248–254.
Cavicchioli, R. (2002). *Astrobiology*, **2**, 281–292.
Cavicchioli, R. (2006). *Nature Rev. Microbiol.* **4**, 331–343.
Cavicchioli, R., Siddiqui, K. S., Andrews, D. & Sowers, K. R. (2002). *Curr. Opin. Biotechnol.* **13**, 253–261.
Chapados, B. R., Hosfield, D. J., Han, S., Qiu, J., Yelent, B., Shen, B. & Tainer, J. A. (2004). *Cell*, **116**, 39–50.
Collaborative Computational Project, Number 4 (1994). *Acta Cryst.* D**50**, 760–763.
D'Amico, S., Collins, T., Marx, J. C., Feller, G. & Gerday, C. (2006). *EMBO Rep.* **7**, 385–389.
Dionne, I., Nookala, R. K., Jackson, S. P., Doherty, A. J. & Bell, S. D. (2003). *Mol. Cell*, **11**, 275–282.
Dore, A. S., Kilkenny, M. L., Jones, S. A., Oliver, A. W., Roe, S. M., Bell, S. D. & Pearl, L. H. (2006). *Nucleic Acids Res.* **34**, 4515–4526.
Franzmann, P. D., Springer, N., Ludwig, W., Conway de Macario, E. & Rode, M. (1992). *Syst. Appl. Microbiol.* **15**, 573–581.
Garcia-Ortega, L., De los Rios, V., Martinez-Ruiz, A., Onaderra, M., Lacadena, J., Martinez del Pozo, A. & Gavilanes, J. G. (2005). *Electrophoresis*, **26**, 3407–3413.
Gerday, C., Aittaleb, M., Bentahir, M., Chessa, J. P., Claverie, P., Collins, T., D'Amico, S., Dumont, J., Garsoux, G., Georlette, D., Hoyoux, A., Lonhienne, T., Meuwis, M. A. & Feller, G. (2000). *Trends Biotechnol.* **18**, 103–107.
Hlinkova, V., Xing, G., Bauer, J., Shin, Y. J., Dionne, I., Rajashankar, K. R., Bell, S. D. & Ling, H. (2008). *Acta Cryst.* D**64**, 941–949.
Kong, X. P., Onrust, R., O'Donnell, M. & Kuriyan, J. (1992). *Cell*, **69**, 425–437.
Krishna, T. S., Kong, X. P., Gary, S., Burgers, P. M. & Kuriyan, J. (1994). *Cell*, **79**, 1233–1243.
Maga, G. & Hubscher, U. (2003). *J. Cell Sci.* **116**, 3051–3060.
Marsic, D., Hughes, R., Byrne-Steele, M. & Ng, J. (2008). *BMC Biotechnol.* **8**, 44.
Matsumiya, S., Ishino, Y. & Morikawa, K. (2001). *Protein Sci.* **10**, 17–23.
Matthews, B. W. (1968). *J. Mol. Biol.* **33**, 491–497.
Moldovan, G. L., Pfander, B. & Jentsch, S. (2007). *Cell*, **129**, 665–679.

Mullis, K. B. & Faloona, F. A. (1987). *Methods Enzymol.* **155**, 335–350.
Naryzhny, S. N., Desouza, L. V., Siu, K. W. & Lee, H. (2006). *Biochem. Cell Biol.* **84**, 669–676.
Naryzhny, S. N. & Lee, H. (2004). *J. Biol. Chem.* **279**, 20194–20199.
Otwinowski, Z. & Minor, W. (1997). *Methods Enzymol.* **276**, 307–326.
Sambrook, J., Fritsch, E. F. & Maniatis, T. (1989). *Molecular Cloning: A Laboratory Manual*, 2nd ed. New York: Cold Spring Harbor Laboratory Press.
Schwarzenbacher, R., Godzik, A., Grzechnik, S. K. & Jaroszewski, L. (2004). *Acta Cryst.* D**60**, 1229–1236.
Stein, N. (2008). *J. Appl. Cryst.* **41**, 641–643.
Warbrick, E. (1998). *Bioessays*, **20**, 195–199.
Warbrick, E. (2000). *Bioessays*, **22**, 997–1006.
Williams, G. J., Johnson, K., Rudolf, J., McMahon, S. A., Carter, L., Oke, M., Liu, H., Taylor, G. L., White, M. F. & Naismith, J. H. (2006). *Acta Cryst.* F**62**, 944–948.